Int. J. Heat Mass Transfer. Vol. 36, No. 1, pp. 119–133, 1993
Printed in Great Britain

0017-9310/93 $5.00 + 0.00

Evaluation of radiation reception factors in a rotary kiln using a modified Monte-Carlo scheme†

C. V. S. MURTY
Chemical Engineering Division, Indian Institute of Chemical Technology, Hyderabad 500 007, India

(*Received* 8 *February* 1990 *and in final form* 10 *February* 1992)

Abstract—Application of the Zone method for the calculation of radiative heat transfer in a rotary kiln is hampered by the nonavailability of the direct exchange area data, essential for the use of the Zone method. Monte-Carlo methods provide a rapid and fairly accurate method of calculating the direct exchange areas in an enclosure and the present study demonstrates the use of a nonstochastic Monte-Carlo procedure for the generation of the exchange area data in a rotary kiln system. The model developed is tested for its accuracy using the data available for the axisymmetric cylindrical system. Exchange areas have been calculated using this model for a wide range of kiln radius–absorption coefficient combinations and percent fills of the solid charge. These data, formulated for conciseness as reception factors, facilitate a rapid evaluation of the radiative interchange in rotary kiln enclosures using the Zone method.

1. INTRODUCTION

IN TODAY'S world, where the energy scene is undergoing rapid transformation with ever-changing prices and fast depleting fossil fuel resources, it has become important to channel our research efforts into areas having a direct impact on energy conservation. Rotary kilns, a specialized form of fired heaters, having application in several areas like cement manufacture, ore reduction, lime calcination, etc. offer ample scope for such an effort. This equipment is highly energy intensive and hence demands efficient methods of design and operation for an optimum utilization of the fuel employed. To achieve this objective, the basic heat transfer processes occurring in the kiln have to be closely investigated. Thermal radiation, being the dominant mode, naturally calls for special attention. Although there is a considerable amount of literature on the mathematical modelling aspects of the rotary kilns, radiation has been rather relegated to the background. There are a few exceptions, however. The radiative interchange in rotary kilns has been modelled by Guruz and Bac [1] using the Monte-Carlo method, by Jenkins and Moles [2] using the Zone method and lastly by Gorog *et al.* [3] using exchange integrals.

Of all the radiation models available, the Zone method is the most accurate for calculating radiative heat transfer in fired heaters. Originally, it had been proposed by Hottel and Cohen [4] for cuboid systems and was later extended to axisymmetrical cylindrical systems by Hottel and Sarofim [5]. Although it has been the most widely used method of its kind, the Zone method suffers from the drawback that it can not be readily applied to systems other than the two mentioned above. This is because the direct exchange area data which are essential for the Zone method are available in a ready-to-use form only for these two systems. The main objective of the present study is to make some amends in this respect, by the generation of the exchange area data for the rotary kiln system to facilitate the use of the Zone method for the prediction of radiative heat exchange in rotary kilns.

Direct exchange areas can be evaluated for the various combinations of surface and gas zones in the enclosure, in several ways. Analytical solutions exist but they are only valid for some simple situations involving zones separated by a transparent medium and hence have limited application. Multiple integration using numerical techniques is the most popular method. The Monte-Carlo methods offer a useful alternative to numerical integration. Richter and Bauersfeld [6] were the first to employ a non-stochastic type Monte-Carlo method for the calculation of direct exchange areas. This was later extended to calculate radiative heat exchange in a heavy fuel oil-fired cylindrical furnace [7]. An essentially similar scheme has been used by Lockwood and Shah [8] in their discrete transfer technique and also by Taniguchi *et al.* [9] in their radiant energy absorption distribution method. Vercammen and Froment [10] proposed a hybrid radiation model, in which a Monte-Carlo method using a random number based decision-making process, is employed for the *in situ* generation of the direct exchange areas, which are processed subsequently as per the Zone method. The present study extends the Monte-Carlo approach of Richter and Bauersfeld [6] for calculating the exchange areas in a rotary kiln and thereby attempts

†IICT Communication No. 2549.

NOMENCLATURE

A	area of a surface element [m^2]
B	characteristic dimension [m]
E	black emissive power [W m^{-2}]
G	gas zone
h	solid bed height [m]
K	absorption coefficient of the medium [m^{-1}]
L	length of the kiln [m]
l	path length [m]
$N\phi$	number of divisions in the polar angle
$N\psi$	average number of divisions in the azimuthal angle
NX	number of subdivisions in the transverse direction
NY	number of subdivisions in the axial direction
NZ	number of subdivisions in the radial direction
PF	percent fill
Q	radiative heat flux [W m^{-2}]
R	kiln radius [m]
S	solid charge zone
sg	surface-to-gas direct exchange area [m^2]
ss	surface-to-surface direct exchange area [m^2]
T	temperature [K]
V	volume of a gas element [m^3]
W	kiln wall zone
x	transverse direction coordinate
y	axial direction coordinate
z	radial direction coordinate.

Greek symbols

ε	emissivity of a surface
θ	angle between the normal to the wall element and the normal to the solid surface [rad]
σ	Stefan–Boltzmann constant
ϕ	polar angle [rad]
ψ	azimuthal angle [rad]
Ω	solid angle [sr].

Subscripts

0	initial
a	absorbed
g	gas
n	new
r	reflected
s	surface
w	wall
v	volume.

Superscript

$'$	pertaining to the inclined wall element.

to demonstrate the utility of Monte-Carlo methods as an alternative to the multiple integration schemes.

The advantages of only selectively using the Monte-Carlo method for the generation of the exchange areas and not for solving the overall radiative transfer problem are not hard to find. This hybrid scheme combines the best features of both the Zone and the Monte-Carlo methods. The flexible nature of the Monte-Carlo approach is made use of for solving once and for all the vexed problem of exchange area determination, without recourse to the tedious multiple integrations. The data generated thereby help in avoiding repetitive calculations to a large extent. The subsequent steps leading to the calculation of radiation fluxes, etc. are problem-specific and can be carried out using the Zone method.

2. SYSTEM CONFIGURATION

A simplified representation of the rotary kiln is given in Fig. 1. The type of model considered is unidimensional, i.e. the kiln is divided axially into several sections. The kiln enclosure is, therefore, made up of four types of zones:

(i) circumferential wall surface (W);
(ii) end surface (E);
(iii) solid charge surface (S) and;
(iv) gas volume (G).

Consequently, a total of 16 sets of zone pair combinations arise, as shown in Table 1. Of these, the 10 sets, which are on and above the diagonal are unique and they have to be compulsorily determined. The rest of the sets, 6 in number, namely, S–E, W–E, W–S, G–E, G–S and G–W may be obtained using the reciprocity relations

$$s_i s_j = s_j s_i \tag{1}$$

and

$$s_i g_j = s_j g_i. \tag{2}$$

The gas-to-gas direct exchange areas, which form part of the unique set, are time-consuming to evaluate and hence may be determined using the conservation criteria

$$\sum_j g_i s_j + \sum_k g_i g_k = 4K_i V_i. \tag{3}$$

3. MONTE-CARLO METHOD

The original Monte-Carlo method discussed by Howell [11] and applied later to practical problems by Steward and Cannon [12] and others [13] envisages the use of random numbers for making decisions with regard to the emission, transmission and absorption of radiation and is plagued as such by statistical errors. Richter [6, 14] proposed an improved Monte-

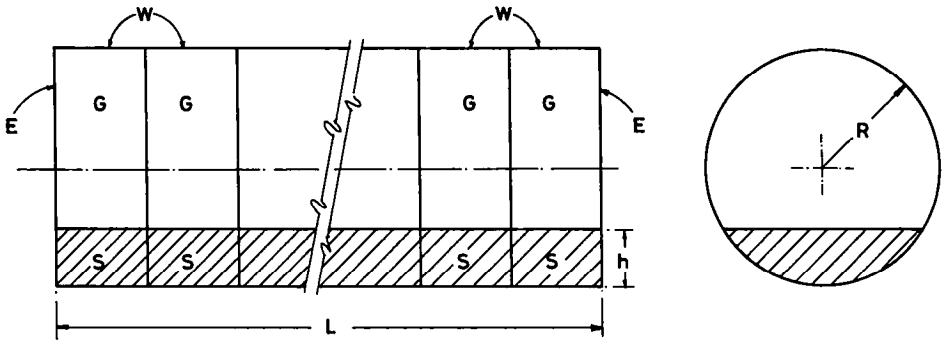

FIG. 1. Rotary kiln configuration.

Carlo scheme to make the method more accurate by minimizing the statistical errors. The method when used for the calculation of radiative transfer in furnaces is nearly deterministic [7], with only the direction a radiation beam would take on reflection at a wall, being decided by random numbers. But, when it is used, as in the present case, for the calculation of direct exchange areas in an enclosure, it is completely deterministic, since reflections do not arise because of the black wall assumption.

Application of the Monte-Carlo method proceeds by assuming that there is only one emitter zone at a time (preferably with emissive power equal to unity) and all the other zones in the enclosure are at a temperature of absolute zero. The emitter zone itself is divided into subelements with the assumption that these elements are small enough to emit radiation isotropically. Size of the subelement is decided by the criterion that further subdivision of the zone does not produce any significant change in the magnitude of the exchange area.

Each subelement of the emitter zone is considered as an emitter at a time and the point of emission of radiation is at the centre of the subelement. The radiative energy flux emitted by the element over the entire space around it (2π steradians for a surface and 4π steradians for a volume) is equally distributed over a fixed number of beams. The directions of the beams are predetermined, with the condition that the solid angles of divergence for the various beams are roughly the same. This is to ensure that there is no bias in any particular direction.

The initial energy flux of a radiation beam emitted by a subelement of a surface i is

$$Q_0 = \varepsilon_i(\sigma T_{s,i}^4/\pi)\cos\phi\,\Delta A_i\Delta\Omega. \quad (4)$$

Likewise, the initial energy of a beam emitted by a volume subelement i is

$$Q_0 = K_i(\sigma T_{g,i}^4/\pi)\Delta V_i\Delta\Omega. \quad (5)$$

The direction in which a beam would travel on release from a surface or volume element is decided by the angles ϕ_0 and ψ_0 associated with the solid angle $\Delta\Omega$. As the beam travels from its point of origin along its path, it loses energy continuously because of attenuation in the medium present in the enclosure. If a ray with an initial energy flux of Q_0 (given by equation (4) or (5) as the case may be) traverses a distance of Δl_j in a volume zone j having an absorption coefficient K_j, its energy is reduced, according to Beer's law, to

$$Q_n = Q_0\exp(-K_j\Delta l_j) \quad (6)$$

and the energy absorbed in the volume zone is

$$Q_{a,v} = Q_0[1-\exp(-K_j\Delta l_j)]. \quad (7)$$

If, on leaving the volume zone j, the beam enters another volume zone k, it will undergo further attenuation. The initial energy flux of the beam will be equal to Q_n given by equation (6). The energy absorbed in each volume zone through which the beam travels can be calculated as above, knowing the path length in each zone and the corresponding absorption coefficient.

Tracing of the beam is continued until either the beam hits a wall or the energy of the beam is reduced to a prefixed fraction of the initial flux. The walls are assumed to be black, so that whatever radiation arrives at the wall is completely absorbed. Thus

$$Q_{a,w} = Q_0\exp(-\Sigma K_m\Delta l_m) \quad (8)$$

the summation $(\Sigma K_m\Delta l_m)$ being carried out for all the volume zones m, through which the ray travels before hitting the wall.

The procedure described above is repeated for all the beams in fixed directions and for all the subelements in the emitter zone. A zone is considered as an emitter only once and the energy fluxes absorbed by the various zones as a result of a plethora of beams passing through them are accumulated in storages

Table 1. Sets of zone pair combinations in the kiln enclosure

	E	S	W	G
E	**End–End**	**End–Solid**	**End–Wall**	**End–Gas**
S	Solid–End	**Solid–Solid**	**Solid–Wall**	**Solid–Gas**
W	Wall–End	Wall–Solid	**Wall–Wall**	**Wall–Gas**
G	Gas–End	Gas–Solid	Gas–Wall	**Gas–Gas**

Bold letters indicate unique sets.

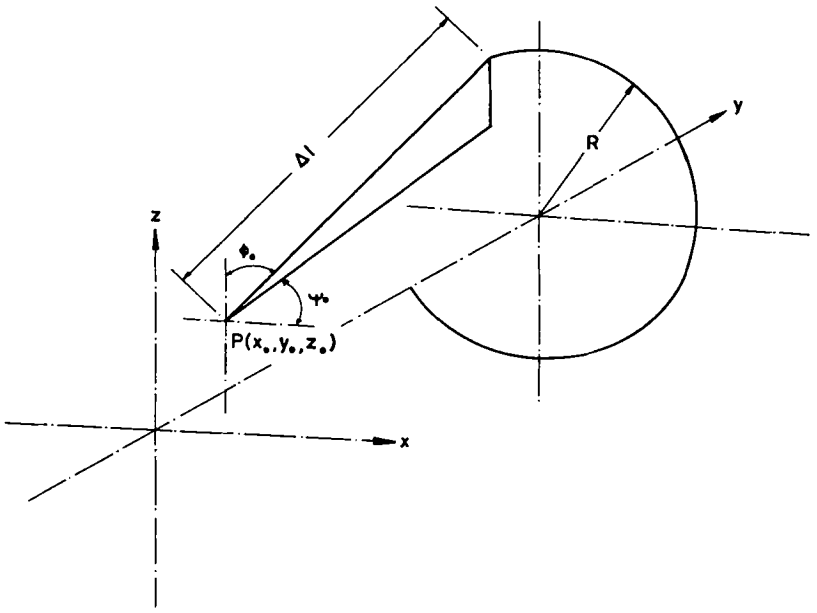

FIG. 2. Path length between the origin of a ray and the point of intersection of the ray with the kiln wall.

assigned to each zone. These yield directly the direct exchange areas for the zone pairs formed between the emitter zone and the other zones, respectively. This follows from the definition of the direct exchange area itself. The method is repeated once with each type of zone as an emitter, to obtain the complete set of exchange areas pertaining to the enclosure.

Path length evaluation

As mentioned earlier, each radiation beam gives away part of its energy to the various volume zones through which it passes on its journey from the point of origin to its ultimate point of absorption. The amount of energy absorbed in any such volume zone depends on the length of the path of the ray in the zone. The evaluation of path lengths is a geometrical problem and is solved based on the intersection of the radiation beams with the planes representing the boundaries of the volume zones. These are of three types: (i) circumferential kiln wall; (ii) solid surface and; (iii) end walls or planes normal to the kiln axis. If the origin of a ray is $P(x_0, y_0, z_0)$ and its direction is defined by the angles ϕ_0 and ψ_0 (Fig. 2), the path length Δl between P and the point of intersection of the ray with the kiln wall is given by

$$\Delta l = [-b \pm \sqrt{(b^2 - 4ac)}]/2a \tag{9}$$

where

$$a = (1 - \sin^2 \phi_0 \sin^2 \psi_0)/2$$

$$b = (x_0 \cos \psi_0 \sin \phi_0 + z_0 \cos \phi_0)$$

$$c = (x_0^2 + z_0^2 - R^2)/2.$$

Similarly, Δl in the case of intersection with the solid surface and the planes normal to the kiln axis is given by

$$\Delta l = (z_1 - z_0)/\cos \phi_0 \tag{10}$$

and

$$\Delta l = (y_1 - y_0)/(\sin \phi_0 \sin \psi_0) \tag{11}$$

respectively. $z = z_1$ represents the solid surface and $y = y_1$ a plane normal to the kiln axis.

Evaluation of the term $\cos \phi$

The term $\cos \phi$ occurring in equation (4) is evaluated based on the polar angle ϕ' measured from the normal to the surface of the emitter. ϕ' for the end walls can be readily expressed in terms of the reference angles ϕ (measured from the normal to the surface of the solid charge, see Fig. 3(b)) and ψ, but not so in the case of the circumferential wall.

The circumferential wall above the solid charge is approximated by a polygon, or in other words, it is divided into a finite number of surface elements (Fig. 3(a)) and the hemispherical space over any one such element is shown in Fig. 3(b). If ϕ' is the polar angle measured from the normal to the inclined wall surface, then $\cos \phi'$ is related to the reference angles ϕ and ψ through

$$\cos \phi' = \cos \phi \cos \theta - \sin \phi \cos \psi \sin \theta \quad \text{for} \quad \theta \leqslant \pi/2 \tag{12}$$

and

$$\cos \phi' = \sin \phi \cos \psi \sin \theta - \cos \phi \cos \theta \quad \text{for} \quad \theta \geqslant \pi/2 \tag{13}$$

where θ is the angle made by the normal to the wall element with the normal to the solid charge.

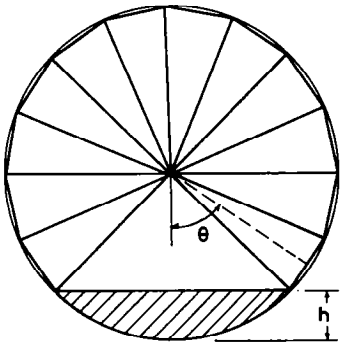

FIG. 3(a). Approximation of the circumferential wall by a polygon.

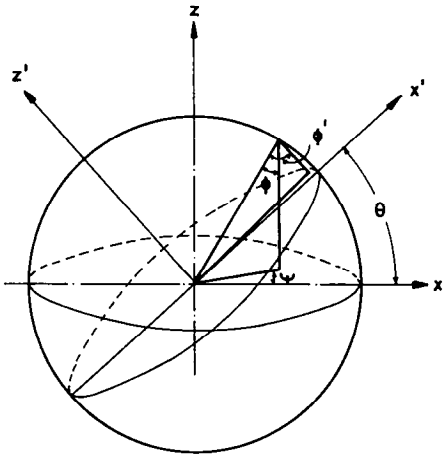

FIG. 3(b). Constitution of the hemispherical space on an inclined wall element.

Proper description of the hemispherical space is essential for determining the direction of a radiation beam in terms of the reference angles ϕ and ψ. For the wall elements, this is slightly complicated because of the fact that the polar angle ϕ is a function of ψ on the base of the hemisphere. The variation of ϕ with ψ is governed for $\theta \leqslant \pi/2$ by

$$0 \leqslant \phi \leqslant \tan^{-1}(\cot\theta \sec\psi)$$
$$\text{for} \quad -\pi/2 \leqslant \psi \leqslant \pi/2 \tag{14}$$
$$0 \leqslant \phi \leqslant \pi/2 + \tan^{-1}[\tan\theta \cos(\psi - \pi)]$$
$$\text{for} \quad \pi/2 \leqslant \psi \leqslant 3\pi/2. \tag{15}$$

Similar relations are obtained for $\pi/2 \leqslant \theta \leqslant \pi$.

4. VALIDATION OF THE PROCEDURE

The method developed must be checked for its validity against any available data, before it is applied to predict the exchange areas in an unknown situation like the rotary kiln. This is accomplished using the data of Erkku [15] for the cylindrical system. End-to-wall, wall-to-wall and other types of exchange areas are calculated using the present procedure for zero solid bed depth for two cases, namely, $KB = 0.0$ and 1.0. A representative sample of these is presented along with Erkku's data in Table 2. A comparison of the two shows that the accuracy of the present method is quite comparable to that of Erkku.

It should be noted that the data generated by Erkku is based on the multiple integration procedure and hence may contain some errors, which are characteristic of the numerical integration scheme used. It is not claimed that the data calculated in the present work are exact, but that they are fairly reliable. The deviations observed from the data of Erkku are tolerable. In a recent study by Murty and Murty [16], it has been shown that errors of this magnitude in the exchange areas do not have any appreciable effect on the Zone method calculations of radiative heat transfer in a fired heater enclosure.

A useful fall-out of the comparison of the calculated exchange areas with the data of Erkku has been the determination of the magnitude of the factors affecting the accuracy of the numerical method, namely, the fineness of subdivision of the zone areas/volumes and also of the hemispherical space surrounding the

Table 2. Comparison of the calculated exchange areas with the data of Erkku (zero solid bed depth : cylindrical furnace case)

Type of exchange area	$KB = 0.0$		$KB = 1.0$	
	Monte-Carlo	Erkku	Monte-Carlo	Erkku
EW 111	0.1954E+01	0.1942E+01	0.1000E+01	0.9953E+00
EW 511	0.6064E−01	0.5856E−01	0.5958E−03	0.5789E−03
EE 411	0.1761E+00	0.1751E+00	0.2891E−02	0.2876E−02
EE 611	0.8397E−01	0.8273E−01	0.1922E−03	0.1898E−03
WW 31	0.4071E+00	0.4095E+00	0.3456E−01	0.3488E−01
WW 84	0.4831E+00	0.4907E+00	0.3925E−04	0.3988E−04
GG 111			0.5409E+01	0.5337E+01
GG 611			0.8696E−03	0.8722E−03
EG 111			0.1791E+01	0.1784E+01
EG 411			0.6748E−02	0.6740E−02
WG 211			0.6394E+00	0.6563E+00
WG 511			0.1519E−02	0.1523E−02

Table 3. Some factors affecting the accuracy of the numerical method

$N\phi$	$N\psi$	NY	NZ	NX
32	18	5	20	10

zones. The values of some such factors employed in the present work are given in Table 3.

5. PRESENTATION OF THE RESULTS

The exchange areas for the various unique zone pair sets have been evaluated in this study for seven cases of KB and five cases of percent fill (PF). KB is the product of the absorption coefficient, K and the characteristic dimension, B. The characteristic dimension selected here is the radius of the kiln. Percent fill is the ratio of the area of the segment formed by the solid charge to the area of the kiln cross-section, expressed in percent. The KB values employed are 0.0, 0.10, 0.25, 0.5, 0.75, 1.0 and 1.25 and the PF values are 5, 15, 25, 35 and 45. These values are expected to cover a wide range of kiln radii, absorption coefficients and solids content normally encountered in practical situations employing rotary kilns.

Only eight axial divisions have been considered in the data generation, as it was found that the radiation beams are left with practically no energy by the time they arrive at the eighth axial position from the point of their origin. The exchange areas have been calculated for the nine unique zone pair sets E–E, E–S, E–W, E–G, S–W, S–G, W–W, W–G and G–G and

Table 4. Reception factors for the E–E set

Percentage fill	Factor code	KB 0.00	0.25	0.50	0.75	1.00	1.25
5	EE1	0.3719E+00	0.2751E+00	0.2040E+00	0.1515E+00	0.1128E+00	0.8412E−01
	EE2	0.1652E+00	0.9602E−01	0.5587E−01	0.3255E−01	0.1899E−01	0.1109E−01
	EE3	0.8738E−01	0.3992E−01	0.1825E−01	0.8350E−02	0.3823E−02	0.1752E−02
	EE4	0.5337E−01	0.1911E−01	0.6844E−02	0.2453E−02	0.8793E−03	0.3154E−03
	EE5	0.3507E−01	0.9830E−02	0.2756E−02	0.7728E−03	0.2168E−03	0.6082E−04
	EE6	0.2498E−01	0.5467E−02	0.1197E−02	0.2621E−03	0.5741E−04	0.1258E−04
	EE7	0.1817E−01	0.3106E−02	0.5312E−03	0.9087E−04	0.1555E−04	0.2660E−05
	EE8	0.1463E−01	0.1950E−02	0.2600E−03	0.3466E−04	0.4623E−05	0.6165E−06
15	EE1	0.3499E+00	0.2595E+00	0.1928E+00	0.1436E+00	0.1071E+00	0.8004E−01
	EE2	0.1518E+00	0.8846E−01	0.5162E−01	0.3015E−01	0.1763E−01	0.1032E−01
	EE3	0.7860E−01	0.3599E−01	0.1649E−01	0.7564E−02	0.3471E−02	0.1594E−02
	EE4	0.4767E−01	0.1710E−01	0.6139E−02	0.2205E−02	0.7921E−03	0.2847E−03
	EE5	0.3192E−01	0.8959E−02	0.2515E−02	0.7062E−03	0.1984E−03	0.5573E−04
	EE6	0.2218E−01	0.4861E−02	0.1066E−02	0.2337E−03	0.5126E−04	0.1125E−04
	EE7	0.1677E−01	0.2869E−02	0.4911E−03	0.8408E−04	0.1440E−04	0.2465E−05
	EE8	0.1291E−01	0.1723E−02	0.2299E−03	0.3069E−04	0.4096E−05	0.5469E−06
25	EE1	0.3247E+00	0.2416E+00	0.1800E+00	0.1344E+00	0.1005E+00	0.7529E−01
	EE2	0.1377E+00	0.8049E−01	0.4710E−01	0.2759E−01	0.1618E−01	0.9494E−02
	EE3	0.7091E−01	0.3255E−01	0.1495E−01	0.6871E−02	0.3160E−02	0.1454E−02
	EE4	0.4248E−01	0.1527E−01	0.5492E−02	0.1976E−02	0.7110E−03	0.2560E−03
	EE5	0.2717E−01	0.7637E−02	0.2148E−02	0.6041E−03	0.1700E−03	0.4783E−04
	EE6	0.1980E−01	0.4345E−02	0.9537E−03	0.2094E−03	0.4597E−04	0.1010E−04
	EE7	0.1458E−01	0.2497E−02	0.4277E−03	0.7328E−04	0.1256E−04	0.2152E−05
	EE8	0.1089E−01	0.1455E−02	0.1945E−03	0.2599E−04	0.3474E−05	0.4645E−06
35	EE1	0.2986E+00	0.2228E+00	0.1665E+00	0.1247E+00	0.9346E−01	0.7017E−01
	EE2	0.1206E+00	0.7071E−01	0.4148E−01	0.2436E−01	0.1432E−01	0.8423E−02
	EE3	0.6239E−01	0.2871E−01	0.1322E−01	0.6092E−02	0.2808E−02	0.1295E−02
	EE4	0.3730E−01	0.1343E−01	0.4839E−02	0.1744E−02	0.6285E−03	0.2266E−03
	EE5	0.2421E−01	0.6817E−02	0.1920E−02	0.5408E−03	0.1524E−03	0.4294E−04
	EE6	0.1722E−01	0.3784E−02	0.8316E−03	0.1828E−03	0.4018E−04	0.8836E−05
	EE7	0.1209E−01	0.2075E−02	0.3560E−03	0.6110E−04	0.1049E−04	0.1800E−05
	EE8	0.9555E−02	0.1279E−02	0.1712E−03	0.2291E−04	0.3068E−05	0.4108E−06
45	EE1	0.2676E+00	0.2004E+00	0.1503E+00	0.1128E+00	0.8484E−01	0.6387E−01
	EE2	0.1049E+00	0.6170E−01	0.3630E−01	0.2138E−01	0.1260E−01	0.7432E−02
	EE3	0.5285E−01	0.2438E−01	0.1125E−01	0.5194E−02	0.2399E−02	0.1109E−02
	EE4	0.3102E−01	0.1120E−01	0.4042E−02	0.1460E−02	0.5273E−03	0.1906E−03
	EE5	0.2034E−01	0.5736E−02	0.1618E−02	0.4564E−03	0.1288E−03	0.3635E−04
	EE6	0.1420E−01	0.3125E−02	0.6881E−03	0.1515E−03	0.3338E−04	0.7353E−05
	EE7	0.1040E−01	0.1788E−02	0.3074E−03	0.5285E−04	0.9086E−05	0.1562E−05
	EE8	0.8328E−02	0.1115E−02	0.1494E−03	0.2000E−04	0.2680E−05	0.3590E−06

these data have been reformulated, for the sake of conciseness, as dimensionless reception factors. The reception factor is defined as the fraction of radiant energy originating from a surface or volume zone that is intercepted directly and absorbed totally by another surface or volume zone. EG6 in Table 7 represents, for instance, the fraction of total radiation emitted by an end refractory which is received at a gas zone that is removed from it by a distance equal to six radii and there absorbed completely. The direct exchange areas for zone pairs formed with a surface zone as the emitter can be obtained from the reception factors by multiplying them with the area of the surface (Tables 4–11). In the case of a volume zone, the multiplying factor is $4KV$, where V is the volume of the gas zone (Table 12).

6. CONCLUSIONS

A non-stochastic type Monte-Carlo method has been used in the present study to generate a comprehensive set of data of radiation reception factors for a rotary kiln system. With the availability of these data, modelling of thermal radiation in rotary kiln enclosures becomes simpler and faster. The Monte-Carlo method is found to be as accurate as the multiple integrations and hence can be regarded as a viable alternative for calculating exchange areas in other geometries.

Table 5. Reception factors for the E–S set

Percentage fill	Factor code	*KB* 0.00	0.25	0.50	0.75	1.00	1.25
5	ES1	0.1181E+00	0.9832E−01	0.8298E−01	0.7092E−01	0.6133E−01	0.5360E−01
	ES2	0.3690E−01	0.2356E−01	0.1515E−01	0.9807E−02	0.6394E−02	0.4196E−02
	ES3	0.1379E−01	0.6996E−02	0.3570E−02	0.1832E−02	0.9450E−03	0.4902E−03
	ES4	0.5898E−02	0.2362E−02	0.9510E−03	0.3849E−03	0.1566E−03	0.6402E−04
	ES5	0.3205E−02	0.1002E−02	0.3145E−03	0.9910E−04	0.3135E−04	0.9957E−05
	ES6	0.1690E−02	0.4144E−03	0.1022E−03	0.2536E−04	0.6330E−05	0.1589E−05
	ES7	0.1331E−02	0.2527E−03	0.4817E−04	0.9222E−05	0.1772E−05	0.3416E−06
	ES8	0.3914E−03	0.5895E−04	0.8901E−05	0.1347E−05	0.2045E−06	0.3114E−07
15	ES1	0.1704E+00	0.1432E+00	0.1218E+00	0.1048E+00	0.9117E−01	0.8007E−01
	ES2	0.4771E−01	0.3082E−01	0.2004E−01	0.1311E−01	0.8636E−02	0.5722E−02
	ES3	0.1756E−01	0.9006E−02	0.4646E−02	0.2410E−02	0.1257E−02	0.6587E−03
	ES4	0.6849E−02	0.2721E−02	0.1087E−02	0.4363E−03	0.1761E−03	0.7142E−04
	ES5	0.3297E−02	0.1064E−02	0.3457E−03	0.1130E−03	0.3716E−04	0.1230E−04
	ES6	0.2426E−02	0.6053E−03	0.1517E−03	0.3822E−04	0.9673E−05	0.2460E−05
	ES7	0.9130E−03	0.1821E−03	0.3647E−04	0.7331E−05	0.1479E−05	0.2995E−06
	ES8	0.1054E−02	0.1642E−03	0.2569E−04	0.4033E−05	0.6352E−06	0.1003E−06
25	ES1	0.2051E+00	0.1739E+00	0.1490E+00	0.1290E+00	0.1128E+00	0.9957E−01
	ES2	0.5014E−01	0.3270E−01	0.2146E−01	0.1417E−01	0.9411E−02	0.6285E−02
	ES3	0.1765E−01	0.9238E−02	0.4865E−02	0.2577E−02	0.1374E−02	0.7361E−03
	ES4	0.7540E−02	0.3079E−02	0.1263E−02	0.5207E−03	0.2156E−03	0.8970E−04
	ES5	0.4159E−02	0.1297E−02	0.4072E−03	0.1288E−03	0.4106E−04	0.1319E−04
	ES6	0.1484E−02	0.3622E−03	0.8872E−04	0.2181E−04	0.5382E−05	0.1332E−05
	ES7	0.1323E−02	0.2554E−03	0.4943E−04	0.9595E−05	0.1867E−05	0.3642E−06
	ES8	0.1045E−02	0.1515E−03	0.2202E−04	0.3211E−05	0.4699E−06	0.6898E−07
35	ES1	0.2333E+00	0.1997E+00	0.1727E+00	0.1507E+00	0.1326E+00	0.1177E+00
	ES2	0.5347E−01	0.3522E−01	0.2334E−01	0.1556E−01	0.1043E−01	0.7028E−02
	ES3	0.1514E−01	0.7857E−02	0.4100E−02	0.2150E−02	0.1133E−02	0.6000E−03
	ES4	0.7144E−02	0.2974E−02	0.1246E−02	0.5247E−03	0.2222E−03	0.9462E−04
	ES5	0.3546E−02	0.1143E−02	0.3693E−03	0.1197E−03	0.3891E−04	0.1268E−04
	ES6	0.1910E−02	0.4723E−03	0.1172E−03	0.2919E−04	0.7297E−05	0.1831E−05
	ES7	0.1515E−02	0.2851E−03	0.5402E−04	0.1031E−04	0.1983E−05	0.3843E−06
	ES8	0.4741E−03	0.7179E−04	0.1090E−04	0.1659E−05	0.2532E−06	0.3874E−07
45	ES1	0.2622E+00	0.2266E+00	0.1975E+00	0.1736E+00	0.1539E+00	0.1374E+00
	ES2	0.5057E−01	0.3361E−01	0.2245E−01	0.1507E−01	0.1017E−01	0.6889E−02
	ES3	0.1500E−01	0.7830E−02	0.4107E−02	0.2165E−02	0.1146E−02	0.6094E−03
	ES4	0.6364E−02	0.2585E−02	0.1056E−02	0.4336E−03	0.1791E−03	0.7435E−04
	ES5	0.2919E−02	0.9147E−03	0.2884E−03	0.9145E−04	0.2917E−04	0.9362E−05
	ES6	0.1627E−02	0.3901E−03	0.9411E−04	0.2284E−04	0.5574E−05	0.1369E−05
	ES7	0.8828E−03	0.1791E−03	0.3654E−04	0.7502E−05	0.1549E−05	0.3216E−06
	ES8	0.6023E−03	0.1008E−03	0.1689E−04	0.2827E−05	0.4734E−06	0.7927E−07

Table 6. Reception factors for the E–W set

Percentage fill	Factor code	*KB* 0.00	0.25	0.50	0.75	1.00	1.25
5	EW1	0.5124E+00	0.4252E+00	0.3581E+00	0.3056E+00	0.2640E+00	0.2308E+00
	EW2	0.1698E+00	0.1078E+00	0.6897E−01	0.4447E−01	0.2890E−01	0.1892E−01
	EW3	0.6406E−01	0.3228E−01	0.1636E−01	0.8346E−02	0.4282E−02	0.2210E−02
	EW4	0.2811E−01	0.1120E−01	0.4487E−02	0.1807E−02	0.7312E−03	0.2975E−03
	EW5	0.1509E−01	0.4728E−02	0.1490E−02	0.4718E−03	0.1502E−03	0.4806E−04
	EW6	0.8407E−02	0.2059E−02	0.5069E−03	0.1255E−03	0.3123E−04	0.7814E−05
	EW7	0.5482E−02	0.1053E−02	0.2034E−03	0.3947E−04	0.7697E−05	0.1508E−05
	EW8	0.3143E−02	0.4734E−03	0.7167E−04	0.1090E−04	0.1667E−05	0.2561E−06
15	EW1	0.4818E+00	0.4021E+00	0.3401E+00	0.2914E+00	0.2527E+00	0.2214E+00
	EW2	0.1504E+00	0.9603E−01	0.6180E−01	0.4007E−01	0.2618E−01	0.1722E−01
	EW3	0.5563E−01	0.2817E−01	0.1435E−01	0.7359E−02	0.3795E−02	0.1969E−02
	EW4	0.2409E−01	0.9614E−02	0.3858E−02	0.1556E−02	0.6311E−03	0.2572E−03
	EW5	0.1245E−01	0.3907E−02	0.1233E−02	0.3910E−03	0.1246E−03	0.3994E−04
	EW6	0.7321E−02	0.1803E−02	0.4464E−03	0.1111E−03	0.2782E−04	0.7000E−05
	EW7	0.4495E−02	0.8661E−03	0.1677E−03	0.3266E−04	0.6389E−05	0.1256E−05
	EW8	0.2804E−02	0.4251E−03	0.6477E−04	0.9916E−05	0.1526E−05	0.2358E−06
25	EW1	0.4721E+00	0.3965E+00	0.3373E+00	0.2904E+00	0.2527E+00	0.2222E+00
	EW2	0.1369E+00	0.8803E−01	0.5704E−01	0.3723E−01	0.2448E−01	0.1620E−01
	EW3	0.4916E−01	0.2502E−01	0.1281E−01	0.6603E−02	0.3423E−02	0.1785E−02
	EW4	0.2089E−01	0.8379E−02	0.3378E−02	0.1369E−02	0.5579E−03	0.2285E−03
	EW5	0.1116E−01	0.3503E−02	0.1105E−02	0.3509E−03	0.1120E−03	0.3592E−04
	EW6	0.5883E−02	0.1451E−02	0.3595E−03	0.8957E−04	0.2242E−04	0.5641E−05
	EW7	0.3899E−02	0.7510E−03	0.1454E−03	0.2827E−04	0.5525E−05	0.1085E−05
	EW8	0.2643E−02	0.4003E−03	0.6090E−04	0.9307E−05	0.1429E−05	0.2203E−06
35	EW1	0.4700E+00	0.3976E+00	0.3404E+00	0.2947E+00	0.2578E+00	0.2276E+00
	EW2	0.1245E+00	0.8067E−01	0.5266E−01	0.3461E−01	0.2291E−01	0.1526E−01
	EW3	0.4312E−01	0.2205E−01	0.1135E−01	0.5874E−02	0.3058E−02	0.1601E−02
	EW4	0.1794E−01	0.7229E−02	0.2929E−02	0.1193E−02	0.4888E−03	0.2012E−03
	EW5	0.9547E−02	0.3024E−02	0.9630E−03	0.3083E−03	0.9919E−04	0.3207E−04
	EW6	0.5077E−02	0.1255E−02	0.3119E−03	0.7791E−04	0.1956E−04	0.4935E−05
	EW7	0.3615E−02	0.6967E−03	0.1350E−03	0.2630E−04	0.5149E−05	0.1013E−05
	EW8	0.2066E−02	0.3142E−03	0.4799E−04	0.7364E−05	0.1135E−05	0.1756E−06
45	EW1	0.4719E+00	0.4028E+00	0.3475E+00	0.3029E+00	0.2665E+00	0.2365E+00
	EW2	0.1121E+00	0.7326E−01	0.4822E−01	0.3195E−01	0.2130E−01	0.1430E−01
	EW3	0.3710E−01	0.1910E−01	0.9889E−02	0.5151E−02	0.2698E−02	0.1421E−02
	EW4	0.1546E−01	0.6245E−02	0.2536E−02	0.1035E−02	0.4249E−03	0.1752E−03
	EW5	0.7763E−02	0.2458E−02	0.7829E−03	0.2507E−03	0.8070E−04	0.2612E−04
	EW6	0.4519E−02	0.1117E−02	0.2777E−03	0.6937E−04	0.1742E−04	0.4397E−05
	EW7	0.2912E−02	0.5641E−03	0.1099E−03	0.2152E−04	0.4239E−05	0.8390E−06
	EW8	0.1472E−02	0.2247E−03	0.3450E−04	0.5324E−05	0.8258E−06	0.1287E−06

Table 7. Reception factors for the E–G set

Percentage fill	Factor code	*KB* 0.10	0.25	0.50	0.75	1.00	1.25
5	EG1	0.8853E−01	0.2037E+00	0.3574E+00	0.4744E+00	0.5642E+00	0.6339E+00
	EG2	0.2437E−01	0.4776E−01	0.6398E−01	0.6470E−01	0.5852E−01	0.4992E−01
	EG3	0.9925E−02	0.1682E−01	0.1769E−01	0.1403E−01	0.9941E−02	0.6641E−02
	EG4	0.4951E−02	0.7249E−02	0.5969E−02	0.3706E−02	0.2056E−02	0.1075E−02
	EG5	0.2807E−02	0.3546E−02	0.2284E−02	0.1109E−02	0.4810E−03	0.1966E−03
	EG6	0.1736E−02	0.1890E−02	0.9497E−03	0.3598E−03	0.1218E−03	0.3884E−04
	EG7	0.1124E−02	0.1055E−02	0.4141E−03	0.1226E−03	0.3240E−04	0.8070E−05
	EG8	0.7717E−03	0.6236E−03	0.1907E−03	0.4395E−04	0.9051E−05	0.1756E−05
15	EG1	0.8557E−01	0.1973E+00	0.3473E+00	0.4622E+00	0.5511E+00	0.6205E+00
	EG2	0.2249E−01	0.4417E−01	0.5938E−01	0.6025E−01	0.5467E−01	0.4677E−01
	EG3	0.9005E−02	0.1529E−01	0.1612E−01	0.1282E−01	0.9112E−02	0.6103E−02
	EG4	0.4473E−02	0.6557E−02	0.5410E−02	0.3366E−02	0.1871E−02	0.9802E−03
	EG5	0.2510E−02	0.3173E−02	0.2046E−02	0.9945E−03	0.4319E−03	0.1767E−03
	EG6	0.1550E−02	0.1690E−02	0.8512E−03	0.3232E−03	0.1096E−03	0.3503E−04
	EG7	0.1004E−02	0.9430E−03	0.3703E−03	0.1096E−03	0.2899E−04	0.7225E−05
	EG8	0.6892E−03	0.5575E−03	0.1708E−03	0.3944E−04	0.8138E−05	0.1582E−05
25	EG1	0.8221E−01	0.1900E+00	0.3356E+00	0.4482E+00	0.5359E+00	0.6049E+00
	EG2	0.2049E−01	0.4034E−01	0.5443E−01	0.5543E−01	0.5046E−01	0.4331E−01
	EG3	0.8046E−02	0.1368E−01	0.1447E−01	0.1154E−01	0.8219E−02	0.5519E−02
	EG4	0.3965E−02	0.5822E−02	0.4818E−02	0.3006E−02	0.1675E−02	0.8798E−03
	EG5	0.2240E−02	0.2835E−02	0.1832E−02	0.8919E−03	0.3880E−03	0.1591E−03
	EG6	0.1356E−02	0.1479E−02	0.7456E−03	0.2833E−03	0.9617E−04	0.3076E−04
	EG7	0.8954E−03	0.8417E−03	0.3311E−03	0.9821E−04	0.2602E−04	0.6496E−05
	EG8	0.6051E−03	0.4900E−03	0.1503E−03	0.3477E−04	0.7185E−05	0.1399E−05
35	EG1	0.7841E−01	0.1817E+00	0.3222E+00	0.4318E+00	0.5180E+00	0.5863E+00
	EG2	0.1834E−01	0.3620E−01	0.4905E−01	0.5014E−01	0.4581E−01	0.3946E−01
	EG3	0.7094E−02	0.1209E−01	0.1281E−01	0.1024E−01	0.7319E−02	0.4926E−02
	EG4	0.3454E−02	0.5077E−02	0.4208E−02	0.2630E−02	0.1468E−02	0.7725E−03
	EG5	0.1932E−02	0.2449E−02	0.1587E−02	0.7748E−03	0.3380E−03	0.1389E−03
	EG6	0.1195E−02	0.1305E−02	0.6591E−03	0.2509E−03	0.8534E−04	0.2734E−04
	EG7	0.7735E−03	0.7276E−03	0.2866E−03	0.8508E−04	0.2256E−04	0.5638E−05
	EG8	0.5063E−03	0.4102E−03	0.1260E−03	0.2916E−04	0.6030E−05	0.1175E−05
45	EG1	0.7400E−01	0.1720E+00	0.3064E+00	0.4124E+00	0.4966E+00	0.5640E+00
	EG2	0.1608E−01	0.3182E−01	0.4330E−01	0.4445E−01	0.4077E−01	0.3525E−01
	EG3	0.6086E−02	0.1039E−01	0.1106E−01	0.8869E−02	0.6356E−02	0.4292E−02
	EG4	0.2955E−02	0.4350E−02	0.3616E−02	0.2266E−02	0.1268E−02	0.6688E−03
	EG5	0.1645E−02	0.2087E−02	0.1353E−02	0.6612E−03	0.2887E−03	0.1187E−03
	EG6	0.1010E−02	0.1104E−02	0.5580E−03	0.2127E−03	0.7242E−04	0.2323E−04
	EG7	0.6310E−03	0.5941E−03	0.2343E−03	0.6967E−04	0.1850E−04	0.4630E−05
	EG8	0.4286E−03	0.3472E−03	0.1066E−03	0.2469E−04	0.5108E−05	0.9955E−06

Table 8. Reception factors for the S–W set

Percentage fill	Factor code	*KB* 0.00	0.25	0.50	0.75	1.00	1.25
5	SW1	0.4148E+00	0.2976E+00	0.2175E+00	0.1621E+00	0.1233E+00	0.9577E−01
	SW2	0.1998E+00	0.1299E+00	0.8547E−01	0.5697E−01	0.3852E−01	0.2644E−01
	SW3	0.5913E−01	0.3214E−01	0.1761E−01	0.9719E−02	0.5407E−02	0.3032E−02
	SW4	0.1929E−01	0.8480E−02	0.3759E−02	0.1680E−02	0.7564E−03	0.3432E−03
	SW5	0.7013E−02	0.2471E−02	0.8773E−03	0.3138E−03	0.1131E−03	0.4103E−04
	SW6	0.3739E−02	0.1029E−02	0.2847E−03	0.7925E−04	0.2220E−04	0.6256E−05
	SW7	0.1235E−02	0.2615E−03	0.5597E−04	0.1211E−04	0.2646E−05	0.5843E−06
	SW8	0.1311E−02	0.2189E−03	0.3677E−04	0.6217E−05	0.1058E−05	0.1813E−06
15	SW1	0.4529E+00	0.3365E+00	0.2542E+00	0.1955E+00	0.1531E+00	0.1221E+00
	SW2	0.1947E+00	0.1307E+00	0.8869E−01	0.6093E−01	0.4241E−01	0.2993E−01
	SW3	0.5217E−01	0.2905E−01	0.1630E−01	0.9216E−02	0.5252E−02	0.3016E−02
	SW4	0.1542E−01	0.6896E−02	0.3109E−02	0.1413E−02	0.6471E−03	0.2986E−03
	SW5	0.6046E−02	0.2131E−02	0.7582E−03	0.2725E−03	0.9886E−04	0.3621E−04
	SW6	0.2138E−02	0.6080E−03	0.1748E−03	0.5081E−04	0.1491E−04	0.4412E−05
	SW7	0.1806E−02	0.3863E−03	0.8316E−04	0.1802E−04	0.3935E−05	0.8654E−06
	SW8	0.4678E−03	0.8464E−04	0.1550E−04	0.2869E−05	0.5360E−06	0.1010E−06
25	SW1	0.4850E+00	0.3709E+00	0.2880E+00	0.2270E+00	0.1817E+00	0.1478E+00
	SW2	0.1917E+00	0.1323E+00	0.9229E−01	0.6513E−01	0.4652E−01	0.3364E−01
	SW3	0.4443E−01	0.2524E−01	0.1446E−01	0.8346E−02	0.4856E−02	0.2847E−02
	SW4	0.1280E−01	0.5823E−02	0.2673E−02	0.1238E−02	0.5780E−03	0.2721E−03
	SW5	0.4532E−02	0.1640E−02	0.5972E−03	0.2189E−03	0.8078E−04	0.2999E−04
	SW6	0.2162E−02	0.5884E−03	0.1616E−03	0.4479E−04	0.1253E−04	0.3536E−05
	SW7	0.9773E−03	0.2254E−03	0.5235E−04	0.1223E−04	0.2873E−05	0.6781E−06
	SW8	0.3331E−03	0.5635E−04	0.9635E−05	0.1665E−05	0.2906E−06	0.5122E−07
35	SW1	0.5179E+00	0.4069E+00	0.3239E+00	0.2611E+00	0.2133E+00	0.1765E+00
	SW2	0.1869E+00	0.1326E+00	0.9507E−01	0.6887E−01	0.5043E−01	0.3734E−01
	SW3	0.3761E−01	0.2176E−01	0.1269E−01	0.7461E−02	0.4421E−02	0.2604E−02
	SW4	0.1007E−01	0.4617E−02	0.2137E−02	0.9973E−03	0.4694E−03	0.2227E−03
	SW5	0.3503E−02	0.1272E−02	0.4677E−03	0.1742E−03	0.6562E−04	0.2498E−04
	SW6	0.1789E−02	0.5157E−03	0.1494E−03	0.4354E−04	0.1275E−04	0.3750E−05
	SW7	0.4315E−03	0.9405E−04	0.2069E−04	0.4592E−05	0.1029E−05	0.2325E−06
	SW8	0.4631E−03	0.7700E−04	0.1294E−04	0.2199E−05	0.3777E−06	0.6555E−07
45	SW1	0.5537E+00	0.4467E+00	0.3643E+00	0.3002E+00	0.2501E+00	0.2106E+00
	SW2	0.1796E+00	0.1310E+00	0.9651E−01	0.7177E−01	0.5389E−01	0.4086E−01
	SW3	0.3098E−01	0.1828E−01	0.1088E−01	0.6531E−02	0.3950E−02	0.2408E−02
	SW4	0.7908E−02	0.3697E−02	0.1742E−02	0.8279E−03	0.3966E−03	0.1914E−03
	SW5	0.2907E−02	0.1035E−02	0.3711E−03	0.1340E−03	0.4873E−04	0.1786E−04
	SW6	0.7627E−03	0.2210E−03	0.6496E−04	0.1935E−04	0.5838E−05	0.1782E−05
	SW7	0.5676E−03	0.1233E−03	0.2704E−04	0.5988E−05	0.1339E−05	0.3022E−06
	SW8	0.6466E−03	0.1113E−03	0.1926E−04	0.3351E−05	0.5864E−06	0.1032E−06

Table 9. Reception factors for the S–G set

Percentage fill	Factor code	*KB* 0.10	0.25	0.50	0.75	1.00	1.25
5	SG1	0.9495E−01	0.2160E+00	0.3731E+00	0.4891E+00	0.5761E+00	0.6426E+00
	SG2	0.2591E−01	0.5418E−01	0.8143E−01	0.9317E−01	0.9612E−01	0.9429E−01
	SG3	0.5626E−02	0.1017E−01	0.1196E−01	0.1064E−01	0.8509E−02	0.6439E−02
	SG4	0.1841E−02	0.2890E−02	0.2682E−02	0.1884E−02	0.1188E−02	0.7085E−03
	SG5	0.7602E−03	0.1032E−02	0.7515E−03	0.4145E−03	0.2052E−03	0.9609E−04
	SG6	0.3657E−03	0.4295E−03	0.2457E−03	0.1064E−03	0.4133E−04	0.1518E−04
	SG7	0.2023E−03	0.2039E−03	0.9038E−04	0.3035E−04	0.9150E−05	0.2611E−05
	SG8	0.1166E−03	0.1020E−03	0.3571E−04	0.9459E−05	0.2247E−05	0.5046E−06
15	SG1	0.8921E−01	0.2042E+00	0.3558E+00	0.4699E+00	0.5569E+00	0.6242E+00
	SG2	0.2286E−01	0.4824E−01	0.7351E−01	0.8514E−01	0.8881E−01	0.8796E−01
	SG3	0.4575E−02	0.8335E−02	0.9916E−02	0.8933E−02	0.7221E−02	0.5523E−02
	SG4	0.1449E−02	0.2287E−02	0.2142E−02	0.1519E−02	0.9660E−03	0.5811E−03
	SG5	0.5927E−03	0.8083E−03	0.5932E−03	0.3296E−03	0.1642E−03	0.7741E−04
	SG6	0.2809E−03	0.3297E−03	0.1885E−03	0.8164E−04	0.3175E−04	0.1169E−04
	SG7	0.1539E−03	0.1567E−03	0.7061E−04	0.2407E−04	0.7358E−05	0.2126E−05
	SG8	0.7803E−04	0.6802E−04	0.2370E−04	0.6257E−05	0.1484E−05	0.3331E−06
25	SG1	0.8382E−01	0.1930E+00	0.3391E+00	0.4510E+00	0.5377E+00	0.6058E+00
	SG2	0.2017E−01	0.4291E−01	0.6622E−01	0.7759E−01	0.8179E−01	0.8177E−01
	SG3	0.3719E−02	0.6818E−02	0.8196E−02	0.7459E−02	0.6090E−02	0.4703E−02
	SG4	0.1140E−02	0.1807E−02	0.1705E−02	0.1218E−02	0.7808E−03	0.4733E−03
	SG5	0.4555E−03	0.6238E−03	0.4612E−03	0.2582E−03	0.1297E−03	0.6159E−04
	SG6	0.2262E−03	0.2668E−03	0.1537E−03	0.6703E−04	0.2621E−04	0.9696E−05
	SG7	0.1064E−03	0.1083E−03	0.4886E−04	0.1671E−04	0.5128E−05	0.1490E−05
	SG8	0.7022E−04	0.6119E−04	0.2130E−04	0.5619E−05	0.1330E−05	0.2982E−06
35	SG1	0.7834E−01	0.1814E+00	0.3215E+00	0.4307E+00	0.5168E+00	0.5853E+00
	SG2	0.1756E−01	0.3766E−01	0.5888E−01	0.6982E−01	0.7441E−01	0.7514E−01
	SG3	0.2954E−02	0.5450E−02	0.6616E−02	0.6080E−02	0.5012E−02	0.3907E−02
	SG4	0.8842E−03	0.1408E−02	0.1338E−02	0.9628E−03	0.6213E−03	0.3792E−03
	SG5	0.3544E−03	0.4855E−03	0.3592E−03	0.2013E−03	0.1013E−03	0.4819E−04
	SG6	0.1599E−03	0.1899E−03	0.1107E−03	0.4887E−04	0.1935E−04	0.7248E−05
	SG7	0.9014E−04	0.9137E−04	0.4092E−04	0.1388E−04	0.4227E−05	0.1218E−05
	SG8	0.6034E−04	0.5279E−04	0.1849E−04	0.4903E−05	0.1167E−05	0.2627E−06
45	SG1	0.7250E−01	0.1689E+00	0.3020E+00	0.4078E+00	0.4926E+00	0.5612E+00
	SG2	0.1495E−01	0.3234E−01	0.5125E−01	0.6156E−01	0.6639E−01	0.6778E−01
	SG3	0.2280E−02	0.4229E−02	0.5183E−02	0.4808E−02	0.4000E−02	0.3146E−02
	SG4	0.6572E−03	0.1051E−02	0.1005E−02	0.7282E−03	0.4731E−03	0.2907E−03
	SG5	0.2635E−03	0.3633E−03	0.2715E−03	0.1535E−03	0.7785E−04	0.3731E−04
	SG6	0.1198E−03	0.1414E−03	0.8161E−04	0.3569E−04	0.1401E−04	0.5206E−05
	SG7	0.7489E−04	0.7623E−04	0.3437E−04	0.1174E−04	0.3596E−05	0.1043E−05
	SG8	0.3646E−04	0.3240E−04	0.1163E−04	0.3160E−05	0.7689E−06	0.1768E−06

Table 10. Reception factors for the W–W set

Percentage fill	Factor code	*KB* 0.00	0.25	0.50	0.75	1.00	1.25
5	WW1	0.2984E+00	0.2095E+00	0.1500E+00	0.1095E+00	0.8174E−01	0.6231E−01
	WW2	0.1541E+00	0.9831E−01	0.6356E−01	0.4171E−01	0.2782E−01	0.1888E−01
	WW3	0.4855E−01	0.2590E−01	0.1393E−01	0.7560E−02	0.4137E−02	0.2284E−02
	WW4	0.1657E−01	0.7188E−02	0.3143E−02	0.1385E−02	0.6153E−03	0.2754E−03
	WW5	0.6612E−02	0.2287E−02	0.7973E−03	0.2801E−03	0.9917E−04	0.3538E−04
	WW6	0.2917E−02	0.7847E−03	0.2134E−03	0.5865E−04	0.1629E−04	0.4570E−05
	WW7	0.1688E−02	0.3676E−03	0.8063E−04	0.1781E−04	0.3961E−05	0.8869E−06
	WW8	0.5209E−03	0.8823E−04	0.1510E−04	0.2612E−05	0.4562E−06	0.8039E−07
15	WW1	0.2537E+00	0.1807E+00	0.1313E+00	0.9738E−01	0.7374E−01	0.5701E−01
	WW2	0.1266E+00	0.8158E−01	0.5332E−01	0.3541E−01	0.2391E−01	0.1644E−01
	WW3	0.3821E−01	0.2048E−01	0.1107E−01	0.6041E−02	0.3326E−02	0.1848E−02
	WW4	0.1310E−01	0.5705E−02	0.2504E−02	0.1108E−02	0.4940E−03	0.2220E−03
	WW5	0.5243E−02	0.1806E−02	0.6263E−03	0.2189E−03	0.7706E−04	0.2734E−04
	WW6	0.2072E−02	0.5577E−03	0.1521E−03	0.4201E−04	0.1175E−04	0.3325E−05
	WW7	0.1551E−02	0.3365E−03	0.7343E−04	0.1612E−04	0.3558E−05	0.7903E−06
	WW8	0.3623E−03	0.6168E−04	0.1064E−04	0.1861E−05	0.3293E−06	0.5895E−07
25	WW1	0.2237E+00	0.1616E+00	0.1190E+00	0.8939E−01	0.6851E−01	0.5354E−01
	WW2	0.1080E+00	0.7039E−01	0.4656E−01	0.3129E−01	0.2139E−01	0.1488E−01
	WW3	0.3108E−01	0.1678E−01	0.9139E−02	0.5024E−02	0.2787E−02	0.1561E−02
	WW4	0.1052E−01	0.4598E−02	0.2026E−02	0.8999E−03	0.4029E−03	0.1818E−03
	WW5	0.4148E−02	0.1429E−02	0.4959E−03	0.1735E−03	0.6124E−04	0.2180E−04
	WW6	0.1571E−02	0.4298E−03	0.1192E−03	0.3345E−04	0.9506E−05	0.2732E−05
	WW7	0.1267E−02	0.2734E−03	0.5935E−04	0.1296E−04	0.2845E−05	0.6286E−06
	WW8	0.2979E−03	0.5030E−04	0.8594E−05	0.1485E−05	0.2597E−06	0.4592E−07
35	WW1	0.1983E+00	0.1453E+00	0.1085E+00	0.8258E−01	0.6402E−01	0.5054E−01
	WW2	0.9229E−01	0.6091E−01	0.4081E−01	0.2778E−01	0.1922E−01	0.1353E−01
	WW3	0.2526E−01	0.1375E−01	0.7557E−02	0.4191E−02	0.2347E−02	0.1327E−02
	WW4	0.8372E−02	0.3678E−02	0.1629E−02	0.7278E−03	0.3278E−03	0.1489E−03
	WW5	0.3267E−02	0.1135E−02	0.3976E−03	0.1405E−03	0.5006E−04	0.1799E−04
	WW6	0.1294E−02	0.3559E−03	0.9904E−04	0.2788E−04	0.7939E−05	0.2284E−05
	WW7	0.9369E−03	0.2018E−03	0.4378E−04	0.9564E−05	0.2104E−05	0.4664E−06
	WW8	0.2534E−03	0.4416E−04	0.7772E−05	0.1381E−05	0.2475E−06	0.4476E−07
45	WW1	0.1759E+00	0.1309E+00	0.9910E−01	0.7636E−01	0.5986E−01	0.4772E−01
	WW2	0.7814E−01	0.5237E−01	0.3562E−01	0.2459E−01	0.1725E−01	0.1230E−01
	WW3	0.2034E−01	0.1119E−01	0.6209E−02	0.3480E−02	0.1968E−02	0.1124E−02
	WW4	0.6570E−02	0.2903E−02	0.1294E−02	0.5817E−03	0.2636E−03	0.1205E−03
	WW5	0.2491E−02	0.8720E−03	0.3079E−03	0.1096E−03	0.3935E−04	0.1424E−04
	WW6	0.9964E−03	0.2737E−03	0.7604E−04	0.2136E−04	0.6068E−05	0.1741E−05
	WW7	0.6744E−03	0.1464E−03	0.3196E−04	0.7027E−05	0.1555E−05	0.3464E−06
	WW8	0.1598E−03	0.2743E−04	0.4765E−05	0.8376E−06	0.1489E−06	0.2674E−07

Table 11. Reception factors for the W–G set

Percentage fill	Factor code	*KB* 0.10	0.25	0.50	0.75	1.00	1.25
5	WG1	0.9698E−01	0.2201E+00	0.3788E+00	0.4952E+00	0.5821E+00	0.6482E+00
	WG2	0.2755E−01	0.5731E−01	0.8545E−01	0.9708E−01	0.9955E−01	0.9714E−01
	WG3	0.6205E−02	0.1116E−01	0.1301E−01	0.1150E−01	0.9129E−02	0.6863E−02
	WG4	0.2076E−02	0.3244E−02	0.2989E−02	0.2086E−02	0.1307E−02	0.7747E−03
	WG5	0.8649E−03	0.1171E−02	0.8486E−03	0.4659E−03	0.2295E−03	0.1069E−04
	WG6	0.4258E−03	0.4972E−03	0.2818E−03	0.1209E−03	0.4658E−04	0.1698E−04
	WG7	0.2186E−03	0.2210E−03	0.9849E−04	0.3324E−04	0.1006E−04	0.2882E−05
	WG8	0.1311E−03	0.1137E−03	0.3924E−04	0.1026E−04	0.2410E−05	0.5358E−06
15	WG1	0.9328E−01	0.2125E+00	0.3676E+00	0.4828E+00	0.5696E+00	0.6362E+00
	WG2	0.2553E−01	0.5336E−01	0.8018E−01	0.9173E−01	0.9467E−01	0.9291E−01
	WG3	0.5517E−02	0.9961E−02	0.1168E−01	0.1038E−01	0.8287E−02	0.6265E−02
	WG4	0.1817E−02	0.2847E−02	0.2635E−02	0.1847E−02	0.1162E−02	0.6915E−03
	WG5	0.7515E−03	0.1019E−02	0.7417E−03	0.4086E−03	0.2019E−03	0.9442E−04
	WG6	0.3703E−03	0.4326E−03	0.2454E−03	0.1054E−03	0.4067E−04	0.1485E−04
	WG7	0.1915E−03	0.1940E−03	0.8674E−04	0.2936E−04	0.8912E−05	0.2559E−05
	WG8	0.1101E−03	0.9568E−04	0.3317E−04	0.8713E−05	0.2055E−05	0.4587E−06
25	WG1	0.8911E−01	0.2038E+00	0.3549E+00	0.4685E+00	0.5552E+00	0.6224E+00
	WG2	0.2330E−01	0.4899E−01	0.7428E−01	0.8569E−01	0.8912E−01	0.8806E−01
	WG3	0.4783E−02	0.8672E−02	0.1024E−01	0.9161E−02	0.7361E−02	0.5600E−02
	WG4	0.1548E−02	0.2432E−02	0.2262E−02	0.1593E−02	0.1007E−02	0.6022E−03
	WG5	0.6368E−03	0.8654E−03	0.6317E−03	0.3491E−03	0.1731E−03	0.8120E−04
	WG6	0.3087E−03	0.3613E−03	0.2056E−03	0.8866E−04	0.3433E−04	0.1258E−04
	WG7	0.1610E−03	0.1634E−03	0.7329E−04	0.2488E−04	0.7577E−05	0.2182E−05
	WG8	0.9226E−04	0.8022E−04	0.2783E−04	0.7312E−05	0.1725E−05	0.3851E−06
35	WG1	0.8438E−01	0.1939E+00	0.3400E+00	0.4516E+00	0.5380E+00	0.6056E+00
	WG2	0.2088E−01	0.4418E−01	0.6768E−01	0.7884E−01	0.8271E−01	0.8239E−01
	WG3	0.4029E−02	0.7337E−02	0.8727E−02	0.7866E−02	0.6366E−02	0.4878E−02
	WG4	0.1277E−02	0.2012E−02	0.1881E−02	0.1332E−02	0.8462E−03	0.5088E−03
	WG5	0.5212E−03	0.7099E−03	0.5201E−03	0.2885E−03	0.1436E−03	0.6764E−04
	WG6	0.2533E−03	0.2971E−03	0.1696E−03	0.7338E−04	0.2849E−04	0.1047E−04
	WG7	0.1320E−03	0.1340E−03	0.6008E−04	0.2040E−04	0.6212E−05	0.1790E−05
	WG8	0.7595E−04	0.6625E−04	0.2309E−04	0.6098E−05	0.1445E−05	0.3242E−06
45	WG1	0.7893E−01	0.1824E+00	0.3224E+00	0.4312E+00	0.5167E+00	0.5847E+00
	WG2	0.1824E−01	0.3889E−01	0.6028E−01	0.7100E−01	0.7525E−01	0.7566E−01
	WG3	0.3269E−02	0.5983E−02	0.7173E−02	0.6517E−02	0.5316E−02	0.4104E−02
	WG4	0.1014E−02	0.1604E−02	0.1508E−02	0.1073E−02	0.6857E−03	0.4145E−03
	WG5	0.4082E−03	0.5575E−03	0.4102E−03	0.2286E−03	0.1143E−03	0.5410E−04
	WG6	0.1960E−03	0.2304E−03	0.1321E−03	0.5739E−04	0.2238E−04	0.8261E−05
	WG7	0.1036E−03	0.1055E−03	0.4749E−04	0.1619E−04	0.4948E−05	0.1430E−05
	WG8	0.5750E−04	0.5017E−04	0.1751E−04	0.4629E−05	0.1099E−05	0.2472E−06

Table 12. Reception factors for the G–G set

Percentage fill	Factor code	KB 0.10	0.25	0.50	0.75	1.00	1.25
5	GG1	0.6149E−01	0.1436E+00	0.2582E+00	0.3504E+00	0.4261E+00	0.4884E+00
	GG2	0.1643E−01	0.3532E−01	0.5549E−01	0.6619E−01	0.7104E−01	0.7229E−01
	GG3	0.4365E−02	0.8041E−02	0.9750E−02	0.8957E−02	0.7389E−02	0.5770E−02
	GG4	0.1853E−02	0.2945E−02	0.2792E−02	0.2005E−02	0.1292E−02	0.7882E−03
	GG5	0.9649E−03	0.1322E−02	0.9784E−03	0.5485E−03	0.2760E−03	0.1314E−03
	GG6	0.5624E−03	0.6640E−03	0.3834E−03	0.1677E−03	0.6585E−04	0.2447E−04
	GG7	0.3563E−03	0.3624E−03	0.1632E−03	0.5567E−04	0.1704E−04	0.4938E−05
	GG8	0.2343E−03	0.2052E−03	0.7203E−04	0.1915E−04	0.4571E−05	0.1033E−05
15	GG1	0.5929E−01	0.1388E+00	0.2505E+00	0.3410E+00	0.4160E+00	0.4776E+00
	GG2	0.1537E−01	0.3314E−01	0.5233E−01	0.6271E−01	0.6758E−01	0.6904E−01
	GG3	0.3969E−02	0.7330E−02	0.8921E−02	0.8227E−02	0.6811E−02	0.5337E−02
	GG4	0.1670E−02	0.2659E−02	0.2527E−02	0.1819E−02	0.1176E−02	0.7189E−03
	GG5	0.8649E−03	0.1187E−02	0.8807E−03	0.4949E−03	0.2496E−03	0.1192E−03
	GG6	0.5064E−03	0.5963E−03	0.3448E−03	0.1511E−03	0.5938E−04	0.2209E−04
	GG7	0.3159E−03	0.3217E−03	0.1451E−03	0.4959E−04	0.1521E−04	0.4416E−05
	GG8	0.2109E−03	0.1848E−03	0.6494E−04	0.1728E−04	0.4129E−05	0.9334E−06
25	GG1	0.5683E−01	0.1335E+00	0.2419E+00	0.3304E+00	0.4038E+00	0.4651E+00
	GG2	0.1422E−01	0.3076E−01	0.4885E−01	0.5885E−01	0.6372E−01	0.6538E−01
	GG3	0.3558E−02	0.6586E−02	0.8049E−02	0.7451E−02	0.6191E−02	0.4869E−02
	GG4	0.1485E−02	0.2368E−02	0.2257E−02	0.1629E−02	0.1055E−02	0.6469E−03
	GG5	0.7653E−03	0.1051E−02	0.7813E−03	0.4399E−03	0.2223E−03	0.1063E−03
	GG6	0.4441E−03	0.5257E−03	0.3048E−03	0.1339E−03	0.5278E−04	0.1969E−04
	GG7	0.2807E−03	0.2859E−03	0.1290E−03	0.4409E−04	0.1353E−04	0.3927E−05
	GG8	0.1860E−03	0.1632E−03	0.5741E−04	0.1503E−04	0.3661E−05	0.8291E−06
35	GG1	0.5411E−01	0.1274E+00	0.2318E+00	0.3179E+00	0.3899E+00	0.4505E+00
	GG2	0.1298E−01	0.2819E−01	0.4503E−01	0.5456E−01	0.5939E−01	0.6124E−01
	GG3	0.3134E−02	0.5816E−02	0.7135E−02	0.6631E−02	0.5531E−02	0.4366E−02
	GG4	0.1297E−02	0.2072E−02	0.1981E−02	0.1434E−02	0.9319E−03	0.5730E−03
	GG5	0.6661E−03	0.9163E−03	0.6824E−03	0.3850E−03	0.1949E−03	0.9336E−04
	GG6	0.3850E−03	0.4559E−03	0.2645E−03	0.1163E−03	0.4588E−04	0.1713E−04
	GG7	0.2443E−03	0.2490E−03	0.1126E−03	0.3857E−04	0.1186E−04	0.3450E−05
	GG8	0.1580E−03	0.1388E−03	0.4900E−04	0.1310E−04	0.3143E−05	0.7137E−06
45	GG1	0.5103E−01	0.1205E+00	0.2203E+00	0.3032E+00	0.3733E+00	0.4328E+00
	GG2	0.1164E−01	0.2538E−01	0.4082E−01	0.4976E−01	0.5450E−01	0.5650E−01
	GG3	0.2700E−02	0.5022E−02	0.6188E−02	0.5774E−02	0.4836E−02	0.3832E−02
	GG4	0.1105E−02	0.1769E−02	0.1696E−02	0.1231E−02	0.8024E−03	0.4949E−03
	GG5	0.5638E−03	0.7767E−03	0.5801E−03	0.3282E−03	0.1666E−03	0.8007E−04
	GG6	0.3283E−03	0.3892E−03	0.2263E−03	0.9965E−04	0.3939E−04	0.1473E−04
	GG7	0.2031E−03	0.2074E−03	0.9407E−04	0.3231E−04	0.9961E−05	0.2906E−05
	GG8	0.1305E−03	0.1147E−03	0.4049E−04	0.1083E−04	0.2600E−05	0.5905E−06

REFERENCES

1. H. K. Guruz and N. Bac, Mathematical modelling of rotary kilns by the Zone method, *Can. J. Chem. Engng* **59**, 540–548 (1981).
2. B. G. Jenkins and F. D. Moles, Modelling of heat transfer from a large enclosed flame in a rotary kiln, *Trans. I. Chem. E.* **59**, 17–25 (1981).
3. J. P. Gorog, J. K. Brimacombe and T. N. Adams, Radiative heat transfer in rotary kilns, *Met. Trans. B* **12B**, 55–70 (1981).
4. H. C. Hottel and E. S. Cohen, Radiant heat exchange in a gas filled enclosure: allowance for non-uniformity of gas temperature, *A.I.Ch.E. Jl* **4**(3), 3–14 (1958).
5. H. C. Hottel and A. F. Sarofim, The effect of gas flow patterns on radiative heat transfer in cylindrical enclosures, *Int. J. Heat Mass Transfer* **8**, 1153–1169 (1965).
6. W. Richter and G. Bauersfeld, Radiation models for use in complete mathematical furnace models. Presented at the Third Members' Conference, International Flame Research Foundation, IJmuiden (1974).
7. W. Richter, G. Fleischhans and C. V. S. Murty, Prediction of radiative heat transfer in a heavy fuel oil flame. Presented at the Joint Meeting of the Heat Transfer and Gas Panels, International Flame Research Foundation, IJmuiden (1978).
8. F. C. Lockwood and N. G. Shah, A new radiation method for incorporation in general combustion prediction procedures, *Proc. 18th Symp. (Int.) Combustion*, Waterloo, p. 1405 (1980).
9. H. Taniguchi, W.-J. Yang, K. Kudo, H. Hayasaka, M. Oguma, A. Kusama, I. Nakamachi and N. Okigami, Radiant transfer in gas filled enclosures by radiant energy absorption distribution method, *Proc. 8th Int. Heat Transfer Conf.*, San Francisco, Vol. 2, pp. 757–762 (1986).
10. A. J. Vercammen and G. F. Froment, An improved zone method using Monte-Carlo techniques for the simulation of radiation in industrial furnaces, *Int. J. Heat Mass Transfer* **23**, 329–337 (1980).
11. J. R. Howell, Application of Monte-Carlo to heat trans-

fer problems. *Advances in Heat Transfer*, Vol. 5, pp. 1–54. Academic Press, London (1968).
12. F. R. Steward and P. Cannon, The calculation of radiative heat flux in a cylindrical furnace using the Monte-Carlo method, *Int. J. Heat Mass Transfer* **14,** 245–262 (1971).
13. P. M. Plehiers and G. F. Froment, Coupled simulation of heat transfer and reaction in a steam reforming furnace, *Chem. Engng Technol.* **12,** 20–26 (1989).
14. W. Richter, Mathematische Modellierung technischer Flammen, Ph.D. Thesis, University of Stuttgart, F.R.G. (1978).
15. H. Erkku, Radiant heat exchange in gas-filled slabs and cylinders, Sc.D. Thesis in Chemical Engineering, Massachusetts Institute of Technology, Cambridge, Massachusetts (1959).
16. C. V. S. Murty and B. S. N. Murty, Significance of exchange area adjustment in Zone modelling, *Int. J. Heat Mass Transfer* **34,** 499–503 (1991).